COPY RIGHT

Title: FUZZY LOGIC CONTROLLER BASED BRUSHLESS DC MOTOR DRIVE FOR UNITY POWER FACTOR USING BRIDGELESS ISOLATED čUK CONVERTER

NADELLA DIVYA SRI, THURAKA SWAMY DAS

Nova Engineering College, Vijayawada;Krishna (Dt); Andhra Pradesh, India.

.

USE THIS BARCODE TO ACCESS YOUR ONLINE PAPER

To Secure Your Paper As Per UGC Guidelines We Are Providing A Electronic Bar Code

FUZZY LOGIC CONTROLLER BASED BRUSHLESS DC MOTOR DRIVE FOR UNITY POWER FACTOR USING BRIDGELESS ISOLATED ČUK CONVERTER

[1]NADELLA DIVYA SRI, [2]THURAKA SWAMY DAS

[1]M-tech Scholar,Department of Electrical & Electronics Engineering,Nova Engineering College, Vijayawada;Krishna (Dt); Andhra Pradesh, India.

[2]Assistant Professor,Department of Electrical & Electronics Engineering,Nova Engineering College, Vijayawada;Krishna (Dt); Andhra Pradesh, India.

[1]sridivya.nadella@gmail.com,[2]swamydas.t@gmail.com

ABSTRACT-Power factor correction (PFC) converters are used to avoid power quality problems at the ac mains. In this work power factor correction (PFC)-based bridgeless isolated Cuk converter-fed brushless dc (BLDC) motor drive. The speed of the BLDC motor is controlled by varying the dc-bus voltage of a voltage source inverter (VSI) which uses a low frequency switching of VSI (electronic commutation of the BLDC motor) for low switching losses. This allows the operation of VSI in fundamental frequency switching to achieve an electronic commutation of the BLDC motor for reduced switching losses. A bridgeless configuration of an isolated Cuk converter is derived for the elimination of the front-end diode bridge rectifier to reduce conduction losses in it. The proposed PFC-based bridgeless isolated Cuk converter is designed to operate in discontinuous inductor current mode to achieve an inherent PFC at the ac mains. The proposed drive is controlled using a single voltage sensor to develop a cost-effective solution. The proposed drive is implemented to achieve a unity power factor at the ac mains for a wide range of speed control and supply voltages. The simulation results are presented by using Matlab/Simulink software.

Index Terms—Bridgeless isolated Cuk converter, brushless dc (BLDC) motor, discontinuous inductor current mode (DICM), power factor correction (PFC), power quality, voltage-source inverter (VSI).

I. INTRODUCTION

Brushless Dc Motor is recommended for many low-cost applications such as household application, industrial, radio controlled cars, positioning and aeromodelling, Heating and ventilation etc., because of its certain characteristics including high efficiency, high torque to weight ratio, more torque per watt, increased reliability, reduced noise, longer life, elimination of ionizing sparks from the commentator, and overall reduction of electromagnetic interference(EMI) etc [1-5]. With no windings on the rotor, they are not subjected to any centrifugal forces, and because the windings are supported by the housing, they can be cooled by conduction, requiring no airflow inside the motor for cooling purposes. The motor's internals can be entirely enclosed and protected from dust, dirt or any other foreign obstacles. There are some draw backs in using conventional Power Factor Correction Methods, by using a Boost converter in Discontinuous Current Mode leads to a high ripple output current. The Buck converter input voltage does not follow the

output voltage in DCM mode and the output voltage is reduced to half which reduces the efficiency [6]. A bridgeless PFCrectifier allows the current to flow through a minimum number of switching devices compared to the conventional Cukrectifier.It also reduces the converter conduction losses and which improves the efficiency and reducing the cost. Abridgeless power factor correction rectifier is introduced to improve the rectifier power density and/or to reduce noisemission via soft-switching techniques or coupled magnetic topologies [7-8].The Cuk converter has several advantages in powerfactor correction applications, such as easy implementation of transformer isolation, natural protection against inrushcurrent occurring at start-up or overload current, lower input current ripple, and less electromagnetic interference(EMI)associated with discontinuous conduction mode topology. Thus, for applications, which require a low current ripple at theinput and output ports of the converter, Cuk converter is efficient [9-10].Brushless Direct Current (BLDC) motors are one of the motor types rapidly gaining popularity. BLDC motors are used inindustries such as Appliances, Automotive, Aerospace, Consumer, Medical, Industrial Automation Equipment andinstrumentation. As the name implies, BLDC motors do not use brushes for commutation; instead, they are electronicallycommutated. BLDC motors have many advantages over brushed DC motors and induction motors [11-14].

II. Operation of PFC Based Bridgeless Isolated CUK Converter

The operation of the proposed PFC converter is classified into two different sections for a line cycle and a switching cycle. Fig.2 shows six different modes of operation. Moreover, Fig.3 shows the associated waveforms of the

PFC converter during a complete switching period.

A.Operation during Complete Line Cycle of Supply Voltage

The proposed bridgeless isolated Cuk converter is designed such that switches S_{w1} and S_{w2} conduct for positive and negative half cycles of supply voltage, respectively.
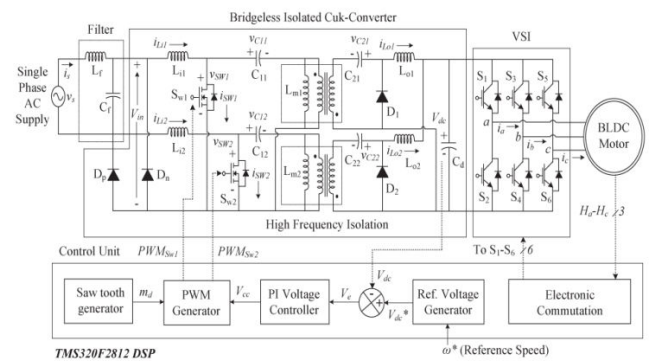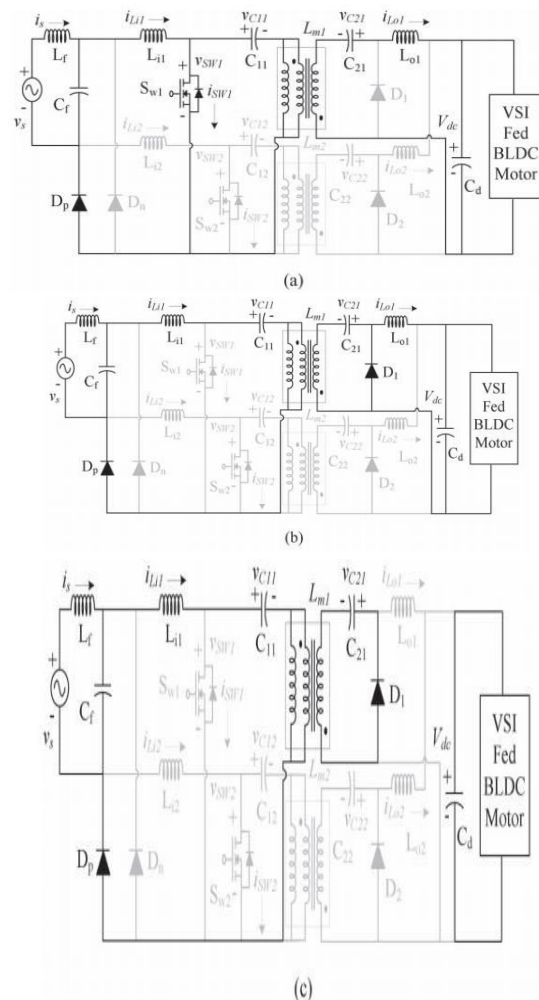

Fig.1. Proposed configuration of a bridgeless isolated Cuk converter-fed BLDC motor drive.

International Journal for Innovative Engineering and Management Research
A Peer Reviewed Open Access International Journal
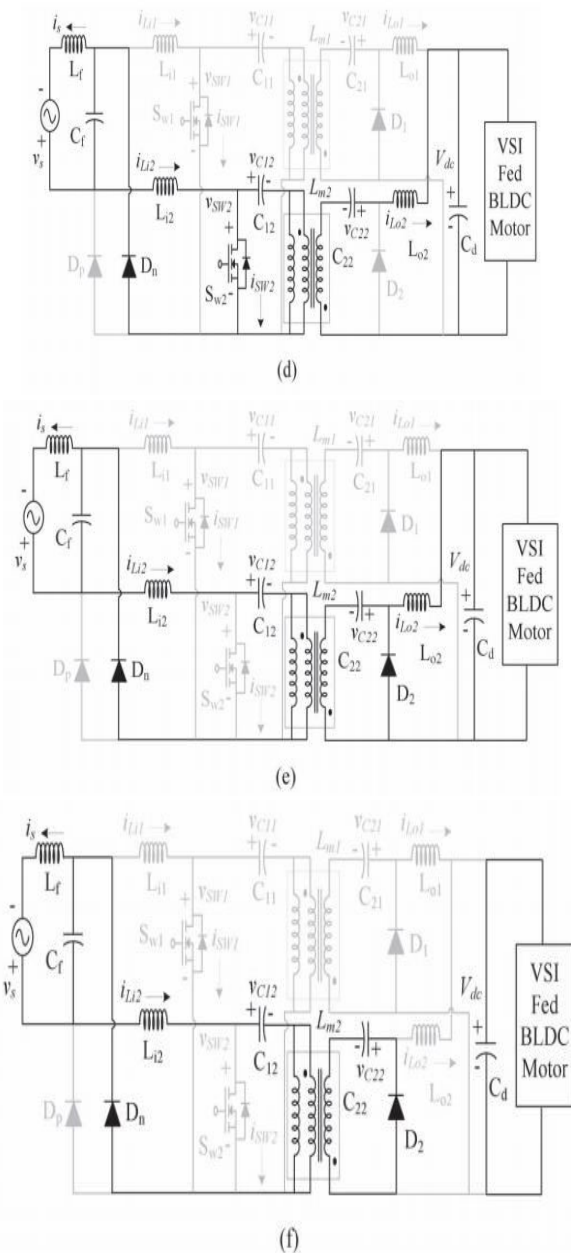www.ijiemr.org

Fig.2. Different modes of operation of bridgeless isolated Cuk converter during (a)–(c) positive and (d)–(f) negative half cycle of supply voltage.

During the positive half cycle of supply voltage, switch S_{w1}, inductors L_{i1} and L_{o1}, intermediate capacitors C_{11} and C_{21}, and diodes D_1 and D_p are in the state of conduction and vice versa for the negative half cycle of supply voltage as shown in Fig.2(a)−(f). As shown in these figures, the proposed PFC converter operates in three different modes during the positive and negative half cycles of

the supply voltage. Moreover, during the DICM operation, the current of output inductors (Lo1 and Lo2) become discontinuous in a switching period.
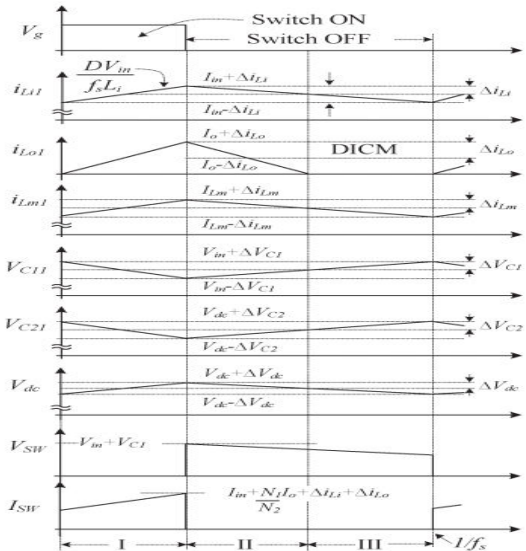

Fig.3. Waveforms of proposed converter in complete switching cycle.

However, the current flowing in the input and magnetizing inductance of the high frequency transformer (HFT) (Li1, Li2, Lm1, and Lm2) and the voltage across the intermediate capacitor (C11, C12, C21, and C22) remain continuous in a complete switching period.

III. Operation during Complete Switching Cycle

Fig.2(a)–(c) shows three modes of operation of a bridgeless isolated Cuk converter in a switching period for the positive half cycle of the supply voltage. Fig.3 shows its associated waveforms in DICM (Lo) mode of operation as follows.

Mode P-I: In this mode, when the switch (Sw1) is turned on, the input inductor (Li1), output inductor (Lo1), and magnetizing inductance of HFT (Lm1) start charging as shown in Fig.2(a). The input side intermediate capacitor (C11) supplies the energy to the HFT, and the output side intermediate capacitor (C21) supplies the required energy to the dc link capacitor as shown in Fig.3.

Mode P-II: When the switch (Sw1) is turned off, the input inductor (Li1), output inductor (Lo1), and magnetizing inductance of HFT(Lm1) start discharging as shown in Fig .2(b). The intermediate capacitors (C11 and C21) charge, and the dc link capacitor (Cd) discharges in this interval as shown in Fig.3.

Mode P-III: During this interval, the output side inductor (Lo1) is completely discharged, and the inputinductor (Li1) and magnetizing inductance of HFT (Lm1) continue to discharge as shown in Fig. 2(c).The output side intermediate capacitor (C21) continues to charge, and the dc link capacitor (Cd) supplies the required energy to the BLDC motor (BLDCM) as shown in Fig.3.In a similar way, the operation for the negative half cycle of the supply voltage is realized.Initially, the intermediate capacitors (C11, C12, C21, and C22) are completely discharged and are charged during the operation of the PFC converter. The voltage across the input side intermediate capacitors (C11 and C12) depends upon the instantaneous input voltage; hence, the initial charging of C11 and C12 is zero. However, the output side intermediate capacitors (C21 and C22) are not completely discharged in a switching period or a half line cycle of the supply voltage due to the voltage maintained at the dc link capacitor (Cd).Moreover, during the operation of the PFC converter in the positive half cycle, the energy storage components on the primary side of the HFT (i.e., Li2, C12 and Lm2) remain in non-conducting state and are completely discharged. However, the energy storage components on the secondary side of HFT (i.e., C22) remain charged at its full voltage due to the unavailability of a discharging path and the presence of the dc link capacitor (Cd).

IV.DESIGN OF BRIDGELESS ISOLATED CUK CONVERTER

A bridgeless isolated Cuk converter is designed to operate in DICM such that the current flowing in the output inductors (Lo1and Lo2) becomes discontinuous in a switching period. A PFC converter of 250 W (P_{max}) is designed for the selected BLDC motor (specifications given in the Appendix). For a wide range of speed, the dc link voltage is controlled from 50 V (V_{dcmin}) to a rated voltage of 130 V (V_{dcmax}) with a supply voltage variation from 170 V (V_{smin}) to 270 V (V_{smax}).The input voltage vs applied to the PFC converter is given as

$$v_s(t) = V_m \mathrm{Sin}(2\pi f_L t) = 220\sqrt{2}\mathrm{Sin}(314t) \quad (1)$$

Where Vm is the peak input voltage (i.e., √2VS) and f_L is the line frequency, i.e., 50 Hz. Now, the instantaneous value of the rectified voltage is given as

$$V_{in}(t) = |V_m \mathrm{Sin}(\omega t)| = \left|220\sqrt{2}\mathrm{Sin}(314t)\right| \quad (2)$$

Where || represents the modulus function.

The output voltage Vdc of a bridgeless isolated Cuk converter which is a buck–boost configuration is given as

$$V_{dc} = \left(\frac{N_2}{N_1}\right) \frac{D}{(1-D)} V_{in} \quad (3)$$

Where D represents the duty ratio and(N2/N1) is the turn's ratio of the HFT which is taken as 1/2 for this application.The instantaneous value of the duty ratio, D (t), depends on the input voltage and dc link voltage. Instantaneous duty ratioD (t) is obtained by substituting (2) in (3) as follows:

$$D(t) = \frac{V_{dc}}{(N_2/N_1)V_{in}(t) + V_{dc}} = \frac{V_{dc}}{(N_2/N_1)|V_m \mathrm{Sin}(\omega t)| + V_{dc}} \quad (4)$$

Since the speed of the BLDC motor is controlled by varying the dc link voltage of VSI, therefore, the instantaneous power Pi is taken as a linear function of Vdc as follows:

$$P_i = \left(\frac{P_{\max}}{V_{\text{dcmax}}} \right) V_{\text{dc}} \qquad (5)$$

Where V_{dcmax} represents the maximum dc link voltage and $P_{\max}$ is the rated power of the PFC converter. Using (5), the minimum power at the minimum dc link voltage of 50 V (V_{dcmin}) is calculated as 96 W ($P_{\min}$). The value of the input inductor to operate in continuous conduction is decided by the amount of permitted ripple current (η) and is given as [12]

$$L_{i1,2} = \frac{V_{\text{in}}(t)D(t)}{\eta I_{\text{in}}(t)f_S} = \frac{1}{\eta f_S} \left(\frac{V_S^2}{P_i} \right) \left(\frac{V_{\text{dc}}}{nV_{in}(t) + V_{\text{dc}}} \right) \qquad (6)$$

Where fs is the switching frequency which is taken as 20 kHz. The maximum inductor ripple current is obtained at the rated condition, i.e., V_{dcmax} ($Pi = P_{\max}$) for a minimum value of the supply voltage (V_{smin}). Hence, the input side inductor is designed at the peak value of the minimum supply voltage ($\sqrt{2}V_{\text{smin}}$).

Using (6), the value of the input side inductors (Li1 and Li2) is calculated as 5.005 mH for a permitted current ripple of 50% (η) of the input current. Hence, the input side inductor of 5 mH is selected for its operation in continuous conduction. The critical value of the output side inductor (L_{oc}) to operate at the boundary of CICM and DICM is given as [12]

$$L_{oc} = \frac{V_{\text{dc}}\{1 - D(t)\}}{2I_{Lo}(t)f_S} = \frac{V_{\text{dc}}D(t)}{2I_{in}(t)f_S}$$
$$= \frac{R_{in}V_{\text{dc}}D(t)}{2V_{in}(t)f_S} = \left(\frac{V_S^2}{P_i} \right) \frac{V_{\text{dc}}}{2V_{in}(t)f_S} \left(\frac{V_{\text{dc}}}{nV_{in}(t) + V_{\text{dc}}} \right) \qquad (7)$$

The maximum current ripple in an inductor occurs at the maximum power and at the minimum value of the supply voltage (i.e., Vsmin). Hence, the output inductor is calculated at the peak of the supply voltage (i.e., $V_{in} = \sqrt{2}V_{\text{smin}}$).

The critical value of output side inductors is calculated at the minimum (Loc50) and

maximum (Loc130) values of dc link voltages using (7) as 459.79 and 811.93 μH, respectively. Hence, the critical value of the output inductor is selected lower than the minimum value, i.e., Loc50, to ensure a discontinuous conduction even at lower values of dc link voltages. Therefore, the output inductor (Lo1 and Lo2) of 70 μH is selected for its operation in discontinuous conduction. The value of the magnetizing inductance of HFT to operate in CICM is decided by the permitted ripple current (ξ) as [11]

$$L_{m1,2} = \frac{V_{\text{dc}}\{1 - D(t)\}}{\Delta I_{Lm}(t)nf_S} = \left(\frac{V_S^2}{P_i} \right) \frac{1}{\xi f_S} \left(\frac{V_{\text{dc}}}{nV_{in}(t) + V_{\text{dc}}} \right) \qquad (8)$$

The maximum current occurs at the maximum dc link voltage (i.e., Pmax) and the minimum supply voltage (i.e., Vsmin). Therefore, the value of the magnetizing inductance (Lm1 and Lm2) for a permitted ripple current (ξ) of 50% is calculated using (8) as 6.006 mH and is selected as 6 mH. The value of input side intermediate capacitors to operate in CCM with a permitted ripple voltage of κ% of VC1 is given as [11]

$$C_{11,12} = \frac{V_{\text{in}}n^2\{D(t)\}^2}{\Delta V_{C1}(t)R_Lf_S\{1 - D(t)\}}$$
$$= \frac{nP_i}{\kappa\left(\sqrt{2}V_s\right)f_S\left(n\sqrt{2}V_s + V_{\text{dc}}\right)} \qquad (9)$$

The input side intermediate capacitors (C11 and C12) are calculated at the maximum value of voltage ripple corresponding to the maximum supply voltage (V_{smax}) and at rated dc link voltage. Now, for a permitted ripple voltage of 25%, the values of C11 and C12 are calculated using (9) as 204 nF and are selected as 220 nF.

The value of output side intermediate capacitors to operate in CCM with a permitted ripple voltage of χ% of VC2 is given as [11]

$$C_{21,22} = \frac{V_{\text{dc}}D(t)}{\Delta V_{C2}(t)R_Lf_S} = \frac{P_i}{\chi V_{\text{dc}}f_S\left(n\sqrt{2}V_s + V_{\text{dc}}\right)} \qquad (10)$$

Now, the maximum ripple voltage occurs at rated condition and at the maximum value of dc link voltage (V_{dcmax}). Hence, the output side intermediate capacitor (C_d) is calculated at the maximum permitted ripple voltage of 10% (χ) of VC21,22 at the maximum (C2c270) and minimum (C2c170) values of supply voltage as 2.99 and 3.84 μF, respectively. Therefore, the output side intermediate capacitors (C21 and C22) are selected higher than C2c85 of the order of 4.4 μF.

The value of the dc link capacitor (C_d) is calculated as [11]

$$C_d = \frac{I_{dc}}{2\omega \Delta V_{dc}} = \left(\frac{P_i}{V_{dc}}\right)\frac{1}{2\omega(\rho V_{dc})} \quad (11)$$

Where ΔV_{dc} represents the permitted ripple in the dc link voltage.

The worst case design occurs for the minimum value of dc link voltage, i.e., 50 V. Hence, for a permitted ripple voltage of 3% (ρ), the value of the dc link capacitor is calculated using (11) as 2038 μF, and it is selected as 2200 μF.

A low-pass LC filter is used to avoid the reflection of higher order harmonics in the supply system. The maximum value of the filter capacitance (C_{max}) is given as [40]

$$C_{max} = \frac{I_m}{\omega_L V_m}\tan(\theta) = \frac{(P_{max}\sqrt{2}/V_s)}{\omega_L \sqrt{2}V_s}\tan(\theta) \quad (12)$$

Where θ is the displacement angle between the fundamental value of the supply voltage and supply current and is taken as 2∘.

The maximum value of the filter capacitor is calculated using (12) as 574.4 nF and is selected as 330 nF.The value of the filter inductor is designed by considering the source impedance (L_s) of 4%–5% of the base impedance. Hence, the additional value of inductance required is given as

$$L_f = L_{req} + L_s \Rightarrow L_{req} = L_f - L_s$$

$$L_{req} = \frac{1}{4\pi^2 f_c^2 C_f} - 0.025\left(\frac{1}{\omega_L}\right)\left(\frac{V_s^2}{P_o}\right) \quad (13)$$

Where fc is the cutoff frequency which is selected such that $f_L < f_c < f_S$. Therefore, fc is

taken as f_S/10.Hence, the value of the filter inductance is calculated using (13) as 3.77 mH.

V. Control of PFC Bridgeless Isolated CUK Converter-Fed BLDC Motor Drive

The control of the proposed BLDC motor drive is divided into two categories of control of the PFC converter for dc link voltage control and control of three-phase VSI for achieving the electronic commutation of the BLDC motor as follows.

A. Control of Front-End PFC Converter

A voltage follower approach is used for the control of the PFC-based bridgeless isolated Cuk converter operating in DICM. This control scheme consists of a reference voltage generator, a voltage error generator, a voltage controller, and a PWM generator. A "Reference Voltage Generator" generates a reference voltage V*dc by multiplying the reference speed (ω∗) with the motor's voltage constant (kv) as

$$V_{dc}* = k_v \omega * \quad (14)$$

The "Voltage Error Generator" compares this reference dc link voltage (V*dc) with the sensed dc link voltage (V_{dc}) to generate an error voltage (Ve) given as

$$V_e(k) = V_{dc}(k) * -V_{dc}(k) \quad (15)$$

Where "k" represents the kth sampling instance. This error voltage Ve is given to a voltage proportional integral (PI) controller to generate a controlled output voltage (Vcc) which is expressed as

$$V_{cc}(k) = V_{cc}(k-1) + K_p\{V_e(k) - V_e(k-1)\} + K_i V_e(k) \quad (16)$$

Finally, the PWM signals for switches Sw1 and Sw2 are generated by comparing the output of the PI controller (Vcc) with the high-frequency saw tooth signal (md) given as

International Journal for Innovative Engineering and Management Research
A Peer Reviewed Open Access International Journal
www.ijiemr.org

$$\text{For } V_S > 0; \begin{cases} \text{if } m_d < V_{cc} \text{ then } PWM_{Sw1} = 'ON' \\ \text{if } m_d \geq V_{cc} \text{ then } PWM_{Sw1} = 'OFF' \end{cases}$$

$$\text{For } V_S < 0; \begin{cases} \text{if } m_d < V_{cc} \text{ then } PWM_{Sw2} = 'ON' \\ \text{if } m_d \geq V_{cc} \text{ then } PWM_{Sw2} = 'OFF' \end{cases} (17)$$

Where PWMSw1 and PWMSw2 represent the gate signals to PFC converter switches Sw_1 and Sw_2, respectively.

In this control algorithm, (17) shows the solid-state switches of the PFC converter operating at half cycles of supply voltages. However, to avoid the sensing of supply voltage for zero crossing detection, only one PWM signal is generated to drive both solid-state switches of the PFC converter, i.e., PWMSw1 =PWMSw2. Moreover, the PFC converter is operating in DCM; therefore, the input current shaping in phase with the supply voltage is obtained inherently, and a unity PF is achieved at the ac mains.

B. Control of BLDC Motor Electronic Commutation

An electronic commutation of the BLDC motor includes the proper switching of the VSI in such a way that a symmetrical dc current is drawn from the dc link capacitor for 120◦ and is placed symmetrically at the center of the back electro-motive force (EMF) of each phase. A Hall-effect position sensor is used to sense the rotor position on a span of 60◦; which is required for the electronic commutation of the BLDC motor. As shown in Fig. 3.1, when two switches of the VSI, i.e., S1 and S4, are in conducting states, a line current iab is drawn from the dc link capacitor whose magnitude depends on the applied dc link voltage (V_{dc}), back EMFs (e_{an} and e_{bn}), resistances (R_a and R_b), and self-inductance and mutual inductance (La, Lb, and M) of stator windings. This current produces an electromagnetic torque (Te) which, in turn, increases the speed of the BLDC motor.

VI INTRODUCTION TO FUZZY LOGIC CONTROLLER

L. A. Zadeh presented the first paper on fuzzy set theory in 1965. Since then, a new language was developed to describe the fuzzy properties of reality, which are very difficult and sometime even impossible to be described using conventional methods. Fuzzy set theory has been widely used in the control area with some application to dc-to-dc converter system. A simple fuzzy logic control is built up by a group of rules based on the human knowledge of system behavior. Matlab/Simulink simulation model is built to study the dynamic behavior of dc-to-dc converter and performance of proposed controllers. Furthermore, design of fuzzy logic controller can provide desirable both small signal and large signal dynamic performance at same time, which is not possible with linear control technique. Thus, fuzzy logic controller has been potential ability to improve the robustness of dc-to-dc converters. The basic scheme of a fuzzy logic controller is shown in Fig 5 and consists of four principal components such as: a fuzzification interface, which converts input data into suitable linguistic values; a knowledge base, which consists of a data base with the necessary linguistic definitions and the control rule set; a decision-making logic which, simulating a human decision process, infer the fuzzy control action from the knowledge of the control rules and linguistic variable definitions; a de-fuzzification interface which yields non fuzzy control action from an inferred fuzzy control action [10].
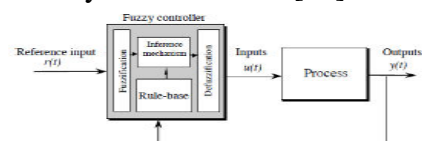

Fig.4. General Structure of the fuzzy logic controller on closed-loop system

International Journal for Innovative Engineering and Management Research
A Peer Reviewed Open Access International Journal
www.ijiemr.org

The fuzzy control systems are based on expert knowledge that converts the human linguistic concepts into an automatic control strategy without any complicated mathematical model [10]. Simulation is performed in buck converter to verify the proposed fuzzy logic controllers.
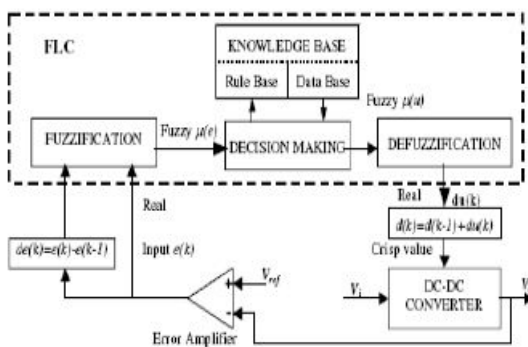

Fig.5. Block diagram of the Fuzzy Logic Controller (FLC) for dc-dc converters

A. Fuzzy Logic Membership Functions:

The dc-dc converter is a nonlinear function of the duty cycle because of the small signal model and its control method was applied to the control of boost converters. Fuzzy controllers do not require an exact mathematical model. Instead, they are designed based on general knowledge of the plant. Fuzzy controllers are designed to adapt to varying operating points. Fuzzy Logic Controller is designed to control the output of boost dc-dc converter using Mamdani style fuzzy inference system. Two input variables, error (e) and change of error (de) are used in this fuzzy logic system. The single output variable (u) is duty cycle of PWM output.
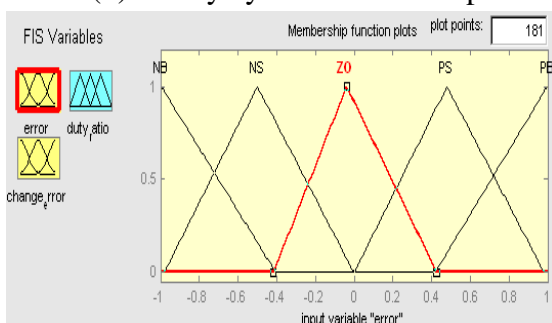
The Membership Function plots of error
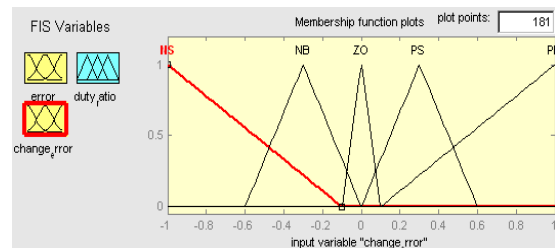
The Membership Function plots of change error
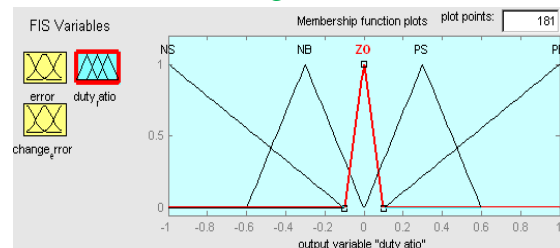
the Membership Function plots of duty ratio

B. Fuzzy Logic Rules:

The objective of this dissertation is to control the output voltage of the boost converter. The error and change of error of the output voltage will be the inputs of fuzzy logic controller. These 2 inputs are divided into five groups; NB: Negative Big, NS: Negative Small, ZO: Zero Area, PS: Positive small and PB: Positive Big and its parameter [10]. These fuzzy control rules for error and change of error can be referred in the table that is shown in Table II as per below:

Table II

Table rules for error and change of error

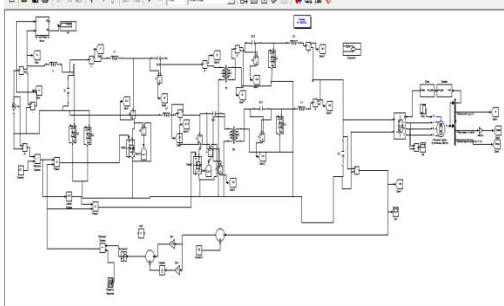| (de) \ (e)	NB	NS	ZO	PS	PB
NB	NB	NB	NB	NS	ZO
NS	NB	NB	NS	ZO	PS
ZO	NB	NS	ZO	PS	PB
PS	NS	ZO	PS	PB	PB
PB	ZO	PS	PB	PB	PB

VII.MATLAB/SIMULATION RESULTS

Fig 6 Matlab/simulation circuit of proposed configuration of a bridgeless isolated Cuk converter-fed BLDC motor drive.
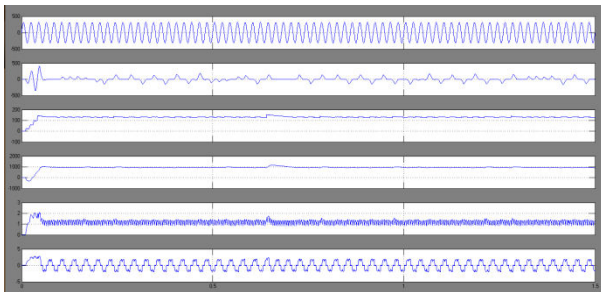

Fig 7 simulation wave form of Test results of the proposed drive during its operation at rated loading condition with dc link voltage as 130 V
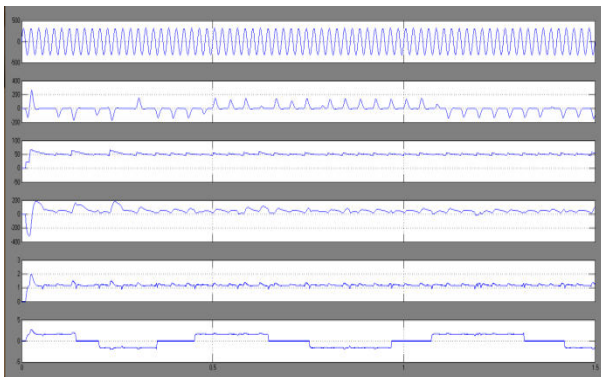

Fig 8 simulation wave form of Test results of the proposed drive during its operation at rated loading condition with dc link voltage as 50 v
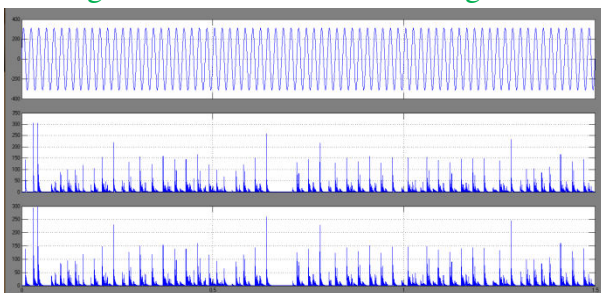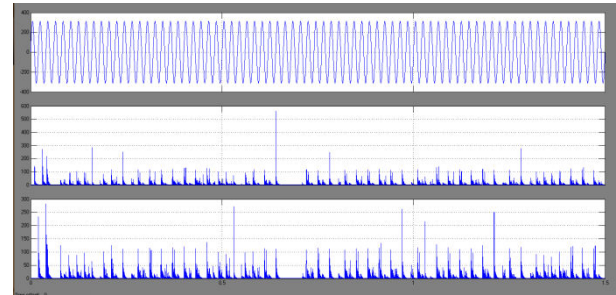

Fig 9 simulation wave form of source voltage

Fig 10 Test results of the proposed drive during its operation at rated condition showing (a) input inductor currents, (b) output inductor currents, and (c) HFT currents
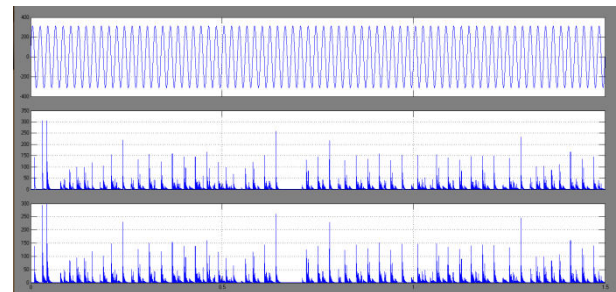

Fig 11 Test results of the proposed drive during its operation at rated condition showing intermediate capacitor voltages (a) VC11 and VC12 and (b) VC21 and VC22.
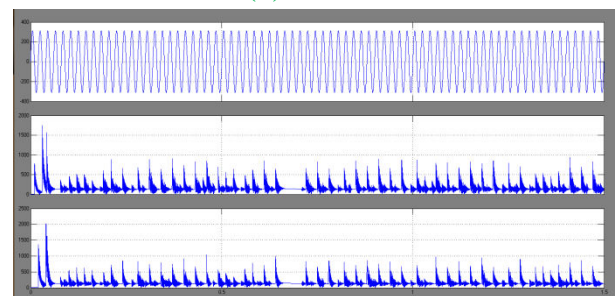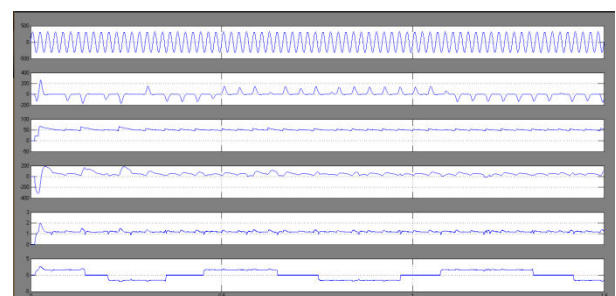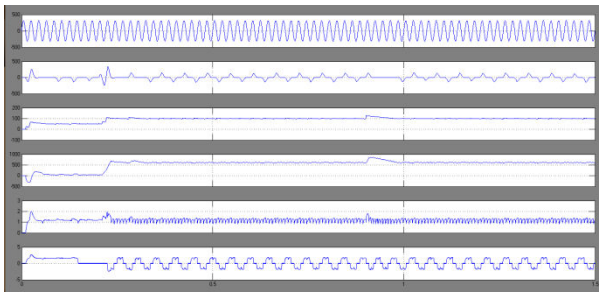

Fig 12 Test results of the proposed drive during its operation at rated condition showing (a) voltage and current stress on PFC converter switches and (b) its enlarged waveforms.
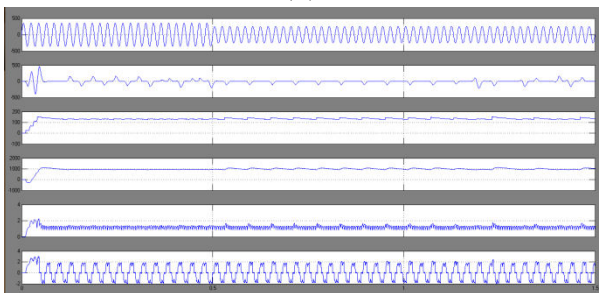

(a)

(b)

(c)

Fig 13 Test results of the proposed drive during (a) starting at dc link voltage of 50 V, (b) speed control corresponding to change in dc link voltage from 50 to 100 V, and (c) supply voltage fluctuation from 250 to 200 V.
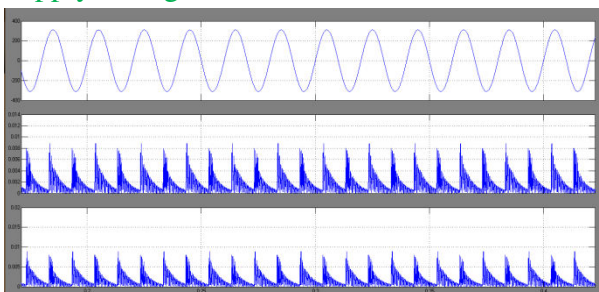

Fig 14 Test results of the proposed drive during its operation at rated condition showing (a) input inductor currents, (b) output inductor currents, and (c) HFT currents with fuzzy logic
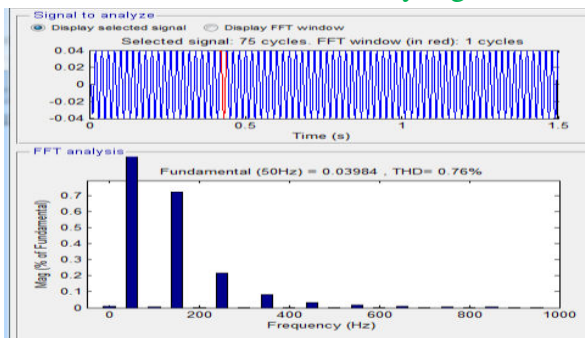

Fig 15 FFT analysis of source current THD with fuzzy logic

VIII. CONCLUSION

The suitable controller for PFC operation of BLDC motor drives has been analyzed. FLC seems to be the best controller in performance improvement of BLDC motor drives for attaining the power factor near to unity. Hence the overall system can be implemented in Air-conditioning System. In the future work, renewable energy like Solar, Fuel cell can be used as the source for the system which is useful to reduce the demand of electricity. It also reduces the pollution and greenhouse effect. Controller performance may further improved by using other intelligent controller. As far as the environment aspects are concerned, this kind of hybrid systems have to be wide spread in order to cover the energy demands and in the way to help reduce the greenhouse gases and the pollution of the environment.

REFERENCES

[1]. VashistBist, Student Member, IEEE, and Bhim Singh, Fellow, IEEE" A Unity Power Factor Bridgeless Isolated Cuk Converter-Fed Brushless DC Motor Drive" IEEE Transactions on Industrial Electronics, Vol. 62, No. 7, July 2015

[2] C. L. Xia, Permanent Magnet Brushless DC Motor Drives and Controls. Beijing, China: Wiley, 2012.

[3] Y. Chen, C. Chiu, Y. Jhang, Z. Tang, and R. Liang, "A driver for the singlephase brushless dc fan motor with hybrid winding structure," IEEE Trans. Ind. Electron., vol. 60, no. 10, pp. 4369–4375, Oct. 2013.

[4] X. Huang, A. Goodman, C. Gerada, Y. Fang, and Q. Lu, "A single sided matrix converter drive for a brushless dc motor in aerospace applications," IEEE Trans. Ind. Electron., vol. 59, no. 9, pp. 3542–3552, Sep. 2012.

[5] J. Moreno, M. E. Ortuzar, and J. W. Dixon, "Energy-management system for a hybrid

electric vehicle, using ultra capacitors and neural networks," IEEE Trans. Ind. Electron., vol. 53, no. 2, pp. 614–623, Apr. 2006.

[6] P. Pillay and R. Krishnan, "Modeling of permanent magnet motor drives," IEEE Trans. Ind. Electron., vol. 35, no. 4, pp. 537–541, Nov. 1988.

[7] H. A. Toliyat and S. Campbell, DSP-Based Electromechanical Motion Control. New York, NY, USA: CRC Press, 2004.

[8] R. Krishnan, Electric Motor Drives: Modeling, Analysis and Control. Bangalore, India: Pearson Education, 2001.

[9] N. Mohan, T. M. Undeland, and W. P. Robbins, Power Electronics: Converters, Applications, and Design. Hoboken, NJ, USA: Wiley, 2009.

[10] Limits for Harmonic Current Emissions (Equipment Input Current $\leq$ 16 A per Phase), International Standard IEC 61000-3-2, 2000.

[11] B. Singh et al., "A review of single-phase improved power quality ac-dc converters," IEEE Trans. Ind. Electron., vol. 50, no. 5, pp. 962–981, Oct. 2003.

[12] B. Singh, S. Singh, A. Chandra, and K. Al-Haddad, "Comprehensive study of single-phase ac-dc power factor corrected converters with highfrequency isolation," IEEE Trans. Ind. Informat., vol. 7, no. 4, pp. 540– 556, Nov. 2011.

[13] V. Bist and B. Singh, "PFC Cuk converter fed BLDC motor drive," IEEE Trans. Power Electron., vol. 30, no. 2, pp. 871–887, Feb. 2015.

[14] R. Martinez and P. N. Enjeti, "A high performance single phase rectifier with input power factor correction," IEEE Trans. Power Electron., vol. 11, no. 2, pp. 311–317, Mar. 1996.

M-tech Scholar Department of Electrical & Electronics Engineering, Nova Engineering College, Vijayawada;
Krishna (Dt); Andhra Pradesh, India.
B-tech: Sri Vasavi Institute of Engineering& Technology. Nandamuru,Pedana Mandal,

Assistant Professor Department of Electrical & Electronics Engineering, Nova Engineering College, Vijayawada;
Krishna (Dt); Andhra Pradesh, India. M-tech: Devineniven kataramana DR Hema sekhar Mic college of technology (Krishna (Dt.) Kanchikacherla) B-tech: Loyola institute of technology and management (Guntur (Dt.) SattenapalliDhullipalla.